Siddiqui, Tauseef; Holopainen, Jari; Viikari, Ville

Ambient Backscattering Transponder with Independently Switchable Rx and Tx Antennas

Published in:
IEEE Sensors Letters

DOI:
10.1109/LSENS.2019.2909184

Published: 01/05/2019

Document Version
Publisher's PDF, also known as Version of record

Please cite the original version:
Siddiqui, T., Holopainen, J., & Viikari, V. (2019). Ambient Backscattering Transponder with Independently Switchable Rx and Tx Antennas. *IEEE Sensors Letters*, *3*(5), Article 3500704.
https://doi.org/10.1109/LSENS.2019.2909184

IEEE Sensors Letters VOL. 3, NO. 5, MAY 2019

Microwave/millimeter wave sensors

Ambient Backscattering Transponder With Independently Switchable Rx and Tx Antennas

Tauseef Ahmad Siddiqui*, Jari Holopainen, and Ville Viikari**

Department of Electronics and Nanoengineering, Aalto University, School of Electrical Engineering, Espoo 02150, Finland.

**Member, IEEE*

***Senior Member, IEEE*

Manuscript received March 15, 2019; accepted March 31, 2019. Date of publication April 3, 2019; date of current version May 7, 2019.

Abstract—This article presents an ambient backscattering transponder with independently beam-switchable receive and transmit antennas. The independently switchable antennas make it possible to collect ambient waves from the direction where they are the strongest and further modulate and redirect the waves toward the receiver possible in a direction other than the ambient source. The transponder consists of patch antennas, circulators, low-power RF switches, and a diode-based modulator.

Index Terms—Microwave/millimeter wave sensors, ambient backscatter, beam steering, Internet-of-Things (IoT), modulation, radio frequency identification (RFID), wireless sensor network (WSN).

I. INTRODUCTION

In recent times, ambient backscatter has been developing as an emerging technology for low-power communication systems [1]. The backscattering communication principle transforms existing ambient RF sources, e.g., cellular base stations, TV towers, FM broadcasting towers, and Wi-Fi access points into both a source of power and an information that is communicated back to the receiver or reader which can be located at different locations [2]. The backscatter transmitter or transponder can transmit data to the backscatter receiver or reader by modulating and reflecting surrounding ambient signals. In spite of the fact that backscatter communication features a great potential for future low-energy communication systems, especially Internet-of-Things (IoT), they are still confronting many challenges. Specifically, unlike the conventional RFID backscatter communication principle, the performance of efficient transmission relies on the ambient RF source location and environment, e.g., indoor or outdoor. Therefore, transponders have to be designed specifically for particular ambient sources in backscattering communication systems.

Today, both RFID and ambient backscattering transponders are solely based on fixed, omnidirectional antennas which do not use the ambient RF energy as effectively as possible. They receive the energy from no particular direction, and they do not redirect the energy to the receiver but scatter it everywhere. An alternative approach to utilize RF energy in efficient manner is to use passive retrodirective wireless sensor, which uses the concept of antenna array by reflecting the received waves back to the direction of incident signal [3]. One of the benefit provided by retrodirectivity are wide ranges in terms of incident angles and in situations, where the location and orientation of the sensor is completely unknown. The complex design circuitry of these retrodirective sensors can draw in power consumption, resulting in shorter read-out distances. In another approach, beam-steerable retrodirective array is also possible, which can reflect away the signal in different directions from the original incident angle [4]. These transponders save energy but are suited only for the backscattering case or for a setup where the ambient source, sensor, and the reader are in fixed directions with respect to each other.

Alternatively, energy-assisted transponders are built in bistatic architecture where transmitter and the reader are not colocated [5]. To achieve longer communication ranges, the components of transponder are powered up by a small battery. For example, in [6], temperature difference between the leaf and the atmosphere is measured to approximate the water stress of a plant. The tag modulates a portion of the ambient frequency modulated (FM) station signals and reflects back to the reader. In this article, we try to leverage a similar approach for ambient backscattering transponders. We can have a transponder that can receive the RF energy from any particular direction and can redirect it to any other particular direction instead of scattering and reflecting the signals everywhere. The beam-steerable transponder can have an increased reading range compared to less-effective isotropic-based transponders. It can also disturb other systems less when the rescattered signals are not radiated omnidirectionally.

This article investigates an ambient backscattering transponder with the functionality of independently switchable Rx and Tx antennas. To the best of the author's knowledge, such designs have not been broadly presented previously and are unique in wireless sensor networks. The novelty of this work is that there is no such transponder in the existing scenario, which could electronically steer the beam in a particular direction. The results show that the proposed approach is a viable candidate to utilize the RF energy in an effective manner. In Section II, the transponder working principle is explained. Section III describes the design process, and Section IV illustrates transponder performance analysis. Finally, the conclusion is given in Section V.

II. WORKING PRINCIPLE OF TRANSPONDER

The transponder is intended to operate at 3.5 GHz. This is an experimental work, and any frequency can be selected for this purpose. Fig. 1 shows schematic layout of transponder illustrating the working principle in which the patch antenna connected to port 1 receives ambient signal from a particular direction then redirects the modulated signal through another patch antenna connected to port 3. For recep-

Corresponding author: Tauseef Ahmad Siddiqui (e-mail: tauseef.siddiqui@aalto.fi).
Associate Editor: D. Uttamchandani.
Digital Object Identifier 10.1109/LSENS.2019.2909184

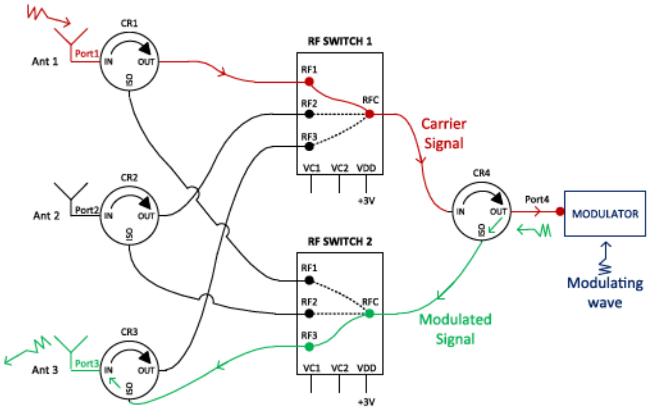

Fig. 1. Schematic illustration of the transponder model.

Table 1. Details of the Components Used in the Transponder.

Parameter	RF switch	RF circulator
Range	0.1 to 6 GHz	3.4 to 3.6 GHz
Insertion loss	0.50 dB	0.25 dB
Isolation	30 dB	20 dB
Return loss	17 dB	20 dB
Input Power	+39 dBm	200 watts
Voltage_{CTL}	1.65 to 3 volts	not applicable
Manufacturer	SKY13373-460LF	MAFRIN0520

tion, any antenna can be chosen and another antenna can be selected for transmission through RF switches, which might also be the same antenna for transmission that received the ambient signal. The patch antennas are selected for this work for the proposed transponder due to their directional radiation pattern. Circulators chosen for this work are passive nonreciprocal three-port device, in which a radio frequency signal entering any port is transmitted to the next port in the rotation direction only. Low-power single pole, triple throw (SP3T) RF switches are selected in this project due to low insertion loss. Switching is controlled by two control voltages, i.e., VC1 and VC2 (see datasheet of RF Switch). Table 1 gives information about the components used in this work.

III. DESIGN PROCESS OF TRANSPONDER

The PCB board is a multilayer structure sandwiched together with a core material (FR4 with dielectric permittivity of $\varepsilon_r = 4.43$ and a loss tangent of $\tan\delta = 0.027$) in between. The RF layers are designed to have 50-Ω transmission lines with width of 0.77 mm. The PCB board is designed using Pads Logic tool software. Fig. 2 shows a photograph of the manufactured transponder prototype along with the dimensions of board. It is noted that the modulator shown in the photograph has been designed in [7]. Patch antennas were designed using simulation software CST. The gain and efficiency of patch antennas were measured in the Starlab facility of Aalto University.

The PCB has four ports, and any port can be used as input and output port except the port 4, which is dedicated for device under test and in our case it is a modulator, which provides independent amplitude and phase modulation as a function of the bias voltage. There is a separate circuitry on the PCB for controlling the switch operations. There is +3-V battery connection to provide power to both RF switches.

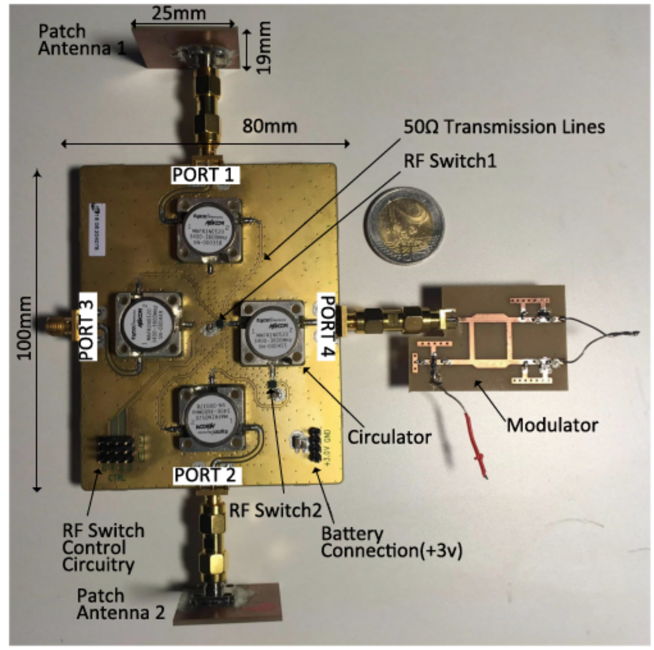

Fig. 2. Transponder prototype.

Table 2. Measured Values Illustrating Board Performance.

Input Port	Output Port	Input Matching (dB)	Transmission Loss (dB)
1	1	-12.2	NA
1	2	-14.2	5.3
1	3	-14.6	5.3
2	1	-13.5	5.2
2	2	-12.4	NA
2	3	-12.3	5.1
3	1	-11.8	5.2
3	2	-13.2	5.3
3	3	-11.2	NA

IV. ANALYSIS OF TRANSPONDER PERFORMANCE

A. Board Performance

The input matching and transmission loss of the PCB when selecting any port as input and output is measured using a vector network analyzer (R&S ZND). Table 2 sums up the information of board performance. When choosing one port for reception and any other port for transmission, it involves three RF circulators (3×0.25 dB) and two RF switches (2×0.50 dB), which corresponds to the transmission loss of 1.75 dB, and the remaining loss of 3.1 to 3.5 dB is contributed by the transmission lines in FR4-based printed circuit board. The total transmission loss of the PCB then becomes approximately 5.1 to 5.3 dB. Obviously, these losses can be further reduced by using a better substrate such as Rogers. The transponder operate in a narrow band due to circulators operational frequency range.

B. Measurement Setup

The operation of the designed transponder is analyzed experimentally; see the measurement setup in Fig. 3. The measurements were performed in the state-of-the-art anechoic chamber of Aalto University to reduce the reflections and disturbances from the surrounding environment. It consists of a signal generator (R&S SMT-06), amplifier (ZVE-8G+), waveform generator (Wavetek 395), spectrum analyzer (Tektronix 2782), and transmitting (Tx) and receiving (Rx) antennas

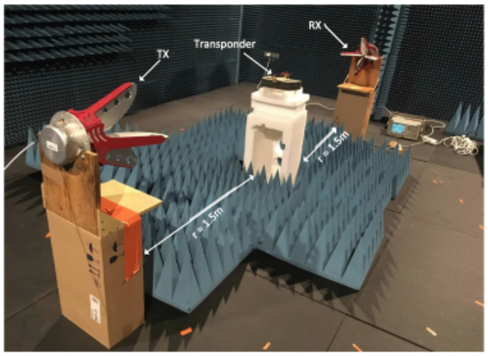

Fig. 3. Measurement setup used in the anechoic chamber. Distance of the transponder from Tx and Rx antennas is the same.

(ETS Lindgren 3164-08 quad-ridged horn antennas). The gain of the horn antennas is approximately 8.8 dBi at 3.5 GHz. The corresponding transponder patch antenna gains are approximately 3.5 dBi. These gains are needed for calculating the path loss in the link budget. The measurement antennas are set to vertical polarization. The transponder is intended to operate in the far field but due to limitations in size of the measurement anechoic chamber, the measurements were taken at a distance of 1.5 m in terms of what can fit inside in the chamber to measure the received power of the proposed transponder. For practical applications, the read-out range of the transponder can be increased by using more transmit power.

The signal generator transmit power of +16 dBm is applied by using amplifier transmit power is increased to approximately +33 dBm. After free space path loss of over 1.5 m distance, the signal is received at the transponder by any port selected as input port using the patch antenna. The carrier signal detected by the transponder transmits to the port 4 of the transponder, which is connected to a modulator. By using wave form generator, the square wave signal of 10 MHz is applied to the modulator for modulation. Any modulating frequency can be chosen, but it should be within the operational bandwidth of the system. The resulting modulated signal of 3.5 GHz ± 10 MHz (3.49 GHz and 3.51 GHz) is generated and transmitted via any other port chosen for transmission. The modulated received power signal is picked up with the receiving antenna and detected with spectrum analyzer.

During measurements, the Tx of the horn antenna is always placed at a fixed point, but the Rx of the horn antenna is moved at different angles in a circular motion to measure the received power and directional pattern of the transponder. Fig. 4 gives the overview of measurement setup illustrating one of the example when port 1 of the transponder is selected as the input port and port 3 as the output port. The distance of the transponder from the Tx and Rx horn antennas is always the same. The value of the measured received power is −58 dBm approximately in the main lobe direction (0° angle in Fig. 4).

C. Link Budget

In order to investigate performance of the proposed transponder, the link budget is calculated. Table 3 displays the link budget for the operation of the transponder. In the link budget, the modulator loss is measured using a spectrum analyzer, and the value of the loss is approximately 16 dB. Transmission loss of PCB from Table 2 is 5.3 dB approximately. The values of calculated and measurement received powers are -60.3 dBm and -58 dBm, respectively, from Table 3. Measurement results show slightly more broadband behavior than the

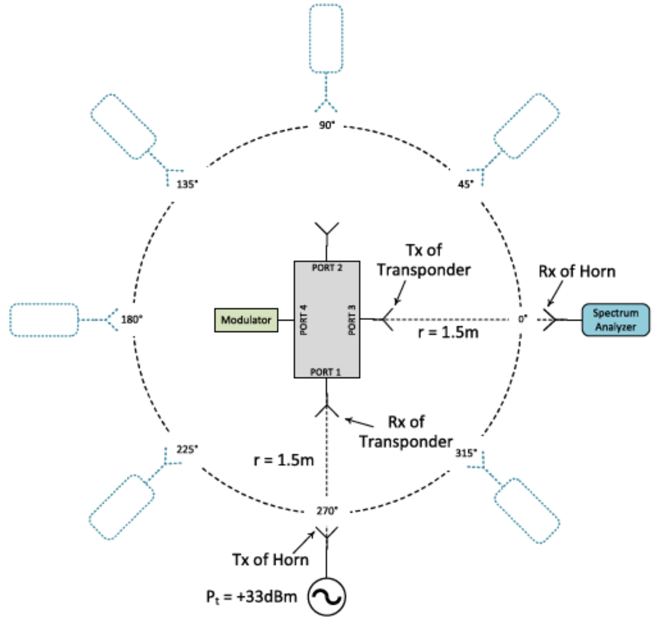

Fig. 4. Measurement illustration when Port 1 is chosen for reception and Port 3 for transmission. Received power measured at different angles to investigate the transponder directional pattern.

Table 3. Link Budget for the Calculated and Measured Received Power at 1.5 m Read-Out Distance of Proposed Transponder.

Parameter	Value
Transmitted Power	(+) 33 dBm
Tx Antenna Cable loss	(-) 1.5 dB
L_{path} from Tx to Transponder (f = 3.5 GHz, G = 3.5 dBi)	(-) 34.5 dB
PCB Transmission loss	(-) 5.3 dB
Modulator loss	(-) 16 dB
L_{path} from Transponder to Rx (f = 3.51 GHz, G = 3.5 dBi)	(-) 34.5 dB
Rx Antenna cable loss	(-) 1.5 dB
Calculated Received Power (Pr)	(-) 60.3 dBm
Measured Received Power (Pr)	(-) 58 dBm

calculations, possibly due to environmental reflections and power received from other directions.

D. Comparison of Directional Pattern With Isotropic Reference

To analyze the directional pattern of our transponder, we compare it with an isotropic transponder. Although there is no isotropic transponder in a real scenario, it can be a good parameter to analyze the directional pattern of the proposed transponder. A new link budget is calculated considering the same cable loss, and modulator loss values were properly taken into account, the PCB transmission loss is not included because we are replacing the proposed transponder with the isotropic-based antenna transponder for comparison. Table 4 displays the link budget for the operation of the isotropic transponder.

In order to analyze the directional pattern of the proposed transponder, the received power is measured in a circular motion, as shown in Fig. 4, at different angles also described in the measurement setup section. Fig. 5 shows the comparison of measured received power of the proposed transponder with the isotropic transponder. The comparison shows that the measured received power is approximately 4 dB better than the traditional isotropic transponder in the main lobe direction and lower in other directions. The received power of the transponder can be further increased if we use high gain patch antennas for

Table 4. Link Budget for the Theoretically Calculated Received Power at 1.5 mr Read-Out Distance of Isotropic Transponder as a Reference Point of View.

Parameter	Value
Transmitted Power	(+) 33 dBm
Tx Antenna Cable loss	(-) 1.5 dB
L_{path} from Tx to Transponder (f = 3.5 GHz, G = 0 dBi)	(-) 38 dB
Modulator loss	(-) 16 dB
L_{path} from Transponder to Rx (f = 3.51 GHz, G = 0 dBi)	(-) 38 dB
Rx Antenna cable loss	(-) 1.5 dB
Isotropic Transponder Calculated Received Power (Pr)	(-) 62 dBm

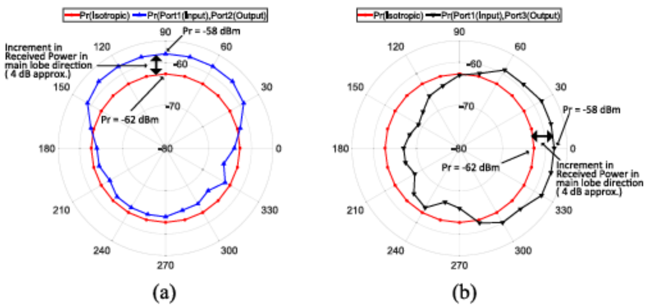

Fig. 5. Measured received power comparison of proposed transponder at different angles with isotropic transponder to analyze directional pattern. (a) Port 1 selected for reception and Port 2 for transmission. (b) Port 1 selected for reception and Port 3 for transmission.

reception and transmission. Patch antennas can have maximum gain up to 6 to 8 dBi, which would subsequently improve the performance of transponder with independent Tx and Rx antennas in terms of received power.

E. Observations on the Transponder Design and Performance

Above, the performance of the proposed transponder of this article is compared with the isotropic antenna-based transponder. The increment in received power is approximately 2.3 (calculated) and 4 dBm (measured) in the main lobe direction in comparison with the isotropic transponder. The main point we are trying to establish here is that if we use a directional high gain antenna with a transponder, it can use the available ambient RF energy in a more efficient manner, and further, the transponder has the capability to steer the beam in a particular direction. Although the steering mechanism is controlled manually at this stage, it can be controlled through a low-power microcontroller which was left out of the study in this work. To achieve the steering capability and increment in received power, we have to compromise with a complex structure (PCB loss, size, components) of the transponder. We cannot get rid of the losses introduced by circulators, switches, and PCB in a complex structure. Compact design with better substrate will decrease the PCB transmission loss, and high-gain patch antennas will improve the performance of transponder subsequently.

V. CONCLUSION

This article has presented the design of a transponder with the capabilities of steering the beam in a particular direction with independent Tx and Rx antennas. The performance of the transponder is investigated both theoretically and experimentally. The main proof of concept in this article is that we can have a directional transponder, which can use the ambient RF energy in a more effective manner. The work presented here is not the final product, but it is the first step toward a better prototype in terms of size, components, and more received power. Future work in this project includes a more compact design, a low loss modulator, and more directive high gain antennas, and the switching operation for selecting the Tx and Rx antennas done by RF switches will be controlled by using a low-power microcontroller.

ACKNOWLEDGMENT

This work was supported by the School of Electrical Engineering, Aalto University, Espoo, Finland, under Project 7205121.

REFERENCES

[1] V. Liu, A. Parks, V. Talla, S. Gollakota, D. Wetherall, and J. R. Smith, "Ambient backscatter: Wireless communication out of thin air," *ACM SIGCOMM Comput. Commun*, vol. 43, no. 4, pp. 39–50, Sep. 2013.

[2] N. Van Huynh , D. T. Hoang, X. Lu, D. Niyato, P. Wang, and D. I. Kim, "Ambient backscatter communications: A contemporary survey," *IEEE Commun. Surv. Tuts*, vol. 20, no. 4, pp. 2889–2922, Oct.–Dec. 2018.

[3] M.-M. Islam, K. Rasilainen, S. Karki, and V. Viikari, "Designing a passive retrodirective wireless sensor," *IEEE Antennas Wireless Propag. Lett.*, vol. 16, pp. 1739–1742, 2017.

[4] M.-G. Christodoulou and D.-P. Chrissoulidis, "Retro-directive array with beam steering capability, made by coupled, self-oscillating mixers," *Microw. Opt. Technol. Lett.*, vol. 49, no. 6, pp. 1303–1309, Jun. 2007.

[5] S. Daskalakis, J. Kimionis, A. Collado, M. Tentzeris, and A. Georgiadis, "Ambient backscatterers using FM broadcasting for low cost and low power wireless applications," *IEEE Trans. Microw. Theory Techn.*, vol. 65, no. 12, pp. 5251–5262, Dec. 2017.

[6] S. Daskalakis, J. Kimionis, A. Collado, M. Tentzeris, and A. Georgiadis, "Ambient FM backscattering for smart agricultural monitoring," in *Proc. IEEE MTT-S Int. Microw. Symp. Dig*, Honolulu, HI, USA, Jun. 2017, pp. 1339–1341.

[7] T. Siddiqui, M. Islam, K. Rasilainen, and V. Viikari, "Transponder utilizing the modulated re-scattering communication principle," in *Proc. XXXIInd Gen. Assem. Sci. Symp. Int. Union Radio Sci.*, INSPEC Accession Number: 17357376, Montreal, QC, Canada, Aug. 19–26, 2017.

[8] A. Wang, V. Iyer, V. Talla, J. R. Smith, and S. Gollakota, "FM backscatter: Enabling connected cities and smart fabrics," in *Proc. USENIX Symp. Netw. Syst. Des. Implement*, Boston, MA, USA, Mar. 2017, pp. 243–258.

[9] K. Finkenzeller, *RFID Handbook*, 2nd ed. Chichester, U.K.: Wiley, 2003.

[10] G. Marrocco, "Pervasive electromagnetics: Sensing paradigms by passive RFID technology," *IEEE Wireless Commun.*, vol. 17, no. 6, pp. 10–17, Dec. 2010.

[11] M.-S. Khan, M.-S. Islam, and H. Deng, "Design of a reconfigurable RFID sensing tag as a generic sensing platform towards the future Internet of Things," *IEEE Internet Things J.*, vol. 1, no. 4, pp. 300–310, Aug. 2014.